Clays and Clay Minerals, Vol. 51, No. 6, 589–598, 2003.

GEOLOGICAL AND MINERALOGICAL CHARACTERIZATION OF ZEOLITES IN LACUSTRINE TUFFS, NGAKURU, TAUPO VOLCANIC ZONE, NEW ZEALAND

R. L. BRATHWAITE*

Institute of Geological and Nuclear Sciences, PO Box 31312, Lower Hutt, New Zealand

Abstract—Mordenite and clinoptilolite have replaced glass shards and pumice in vitric tuffs that are the products of ash fall-out into lake basins of late Quaternary age in the Taupo Volcanic Zone. The vitric tuffs are intercalated with siltstone and diatomite and overlie pumice-rich, rhyolitic ignimbrite. A Zr/TiO_2-Nb/Y immobile element ratio plot indicates that the vitric tuffs, like the ignimbrite, are of rhyolitic composition. X-ray diffraction and scanning electron microscopy studies indicate that the mordenite and clinoptilolite are accompanied by authigenic K-feldspar and Opal-CT. The zeolites and other authigenic minerals are very fine grained (<10 μm), with open meshes of acicular mordenite crystals that result in low densities (0.7–1.0 g cm^{-3}) in mordenite-rich tuffs. From Pearce element ratio analysis of whole-rock chemical analyses, only Na and K appear to have been mobilized during alteration. The zeolite deposits are associated with sinter, hydrothermal eruption breccias and silicified fault breccias that represent surface or near-surface manifestations of geothermal activity. Plant material extracted from a sinter overlying one of the deposits has a ^{14}C age of 8498±60 BP, which is interpreted to be the age of zeolite deposition for this deposit. Mordenite and clinoptilolite occur in the lower-*T* (60–110ºC) parts of some active or recently active geothermal systems elsewhere in the Taupo Volcanic Zone. The main fluid in these systems is weakly saline (alkali-chloride) water heated by geothermal activity. The Ngakuru zeolite deposits are interpreted as the products of the reaction of vitric tuffs with this type of water in the near-surface part of recently active geothermal systems.

Key Words—Clinoptilolite, Diatomite, Geothermal Systems, Ignimbrite, Late Quaternary, Mordenite, Opal-CT, Sinter, Vitric Tuffs.

INTRODUCTION

Mordenite and clinoptilolite deposits of economic value occur within a sequence of late-Quaternary lake sediments and ignimbrites in the Ngakuru area within the Taupo Volcanic Zone (TVZ) on the North Island of New Zealand (Figure 1). Mordenite, clinoptilolite, laumontite and wairakite have previously been recorded as hydrothermal alteration products of vitric ignimbrites in some of the active and extinct geothermal fields of the TVZ (Steiner, 1953, 1977; Henneberger and Browne, 1988; Simmons *et al.*, 1992). The mordenite and clinoptilolite deposits in vitric-rich lake sediments have only recently been discovered (Roberts, 1997). Three of these deposits near Ngakuru are being worked and current uses include: (1) adsorbents for soaking up oil/chemical spills and animal wastes; (2) water treatment and filters; and (3) conditioners for sports turf and slow-release fertilizer (Mowatt, 2000).

This paper focuses on the geology, mineralogy, occurrence and origin of the Ngakuru zeolite deposits. The findings are intended for use in evaluating economic applications of the zeolite deposits and in exploration for new deposits.

* E-mail address of corresponding author:
b.brathwaite@gns.cri. nz
DOI: 10.1346/CCMN.2003.0510601

GEOLOGICAL SETTING

Regional geology

The Ngakuru area lies within the Taupo Volcanic Zone (TVZ), an active 25–50 km wide volcano-tectonic zone along the Pacific-Australian plate boundary in the North Island of New Zealand. The TVZ contains volcanic rocks <2 Ma old, erupted from a number of centers within the zone. The volcanic rocks are calc-alkaline in composition with voluminous tephras, ignimbrites and rhyolites, and minor dacite and andesite lavas (Wilson *et al.*, 1995). Numerous lakes associated with large caldera volcanoes (*e.g.* Lake Taupo), are depocenters for volcanic-derived sands and silts. Extensive lakes also existed during the late Quaternary, as indicated by occurrences of diatomaceous silts, pumice sands and intercalated tuffs of the Huka Group (Grindley, 1960) in drill holes and rare surface outcrops over an area of 110 by 40 km (Smith *et al.*, 1993; Manville, 2001).

The TVZ is a region of elevated heat flow, predominantly by hydrothermal convection (Bibby *et al.*, 1995) from thin crust (15 km) intruded by magma. The convective heat flow is manifested by 17 high-temperature geothermal fields, each 10–20 km^2 in area, which are mainly confined to the currently active eastern side of the TVZ. A number of extinct geothermal systems have been recognized in the western side of the TVZ, including one at Ohakuri, 14 km southwest of Ngakuru. A still weakly active geothermal system occurs

at Horohoro in the northwestern part of the Ngakuru area (Figure 1).

Geology of the Ngakuru area

The Ngakuru area lies within the Ngakuru and Guthrie grabens, a northeast-trending fault belt on the western side of the TVZ. The oldest rocks exposed are ignimbrites and rhyolites, dated at 330–220 ka (Wilson *et al.*, 1995) (Figure 1). The predominant lithology is non-welded pumice lapilli tuff of the Ohakuri Ignimbrite. This tuff contains pumice clasts and broken crystals of andesine, quartz, augite, titanomagnetite, hornblende, plus rare biotite, apatite and zircon in a vitroclastic matrix (Henneberger and Browne, 1988; Langridge, 1990).

The Ohakuri Ignimbrite is overlain by lacustrine sediments of the Huka Group, which in this area consists of the Ngakuru Formation, a 100–300 m thick sequence of siltstone, vitric tuff, pumiceous tuff, diatomite, sandstone and conglomerate (Langridge, 1990). The older part of the sequence occurs in the Guthrie Graben and is overlain by the Earthquake Flat Pyroclastics, which have a K-Ar date of 64 ka (Wilson *et al.*, 1992; Villamor and Berryman, 2001). The Earthquake Flat Pyroclastics comprises rhyolitic pyroclastic flows with interbedded surge and airfall deposits. They were erupted from vents ~15 km northeast of Ngakuru and would probably have contributed large volumes of airfall ash to the lacustrine beds of the Ngakuru Formation. In the Ngakuru Graben the upper part of Ngakuru Formation is preserved, as indicated from ^{14}C dates of ~20 ka and >47 ka in samples of carbonaceous material near the top and 30 m below the top of the sequence, respectively (Villamor and Berryman, 2001). A horst block of Ohakuri Ignimbrite (Figure 1) separates these older and younger units of the Ngakuru Formation.

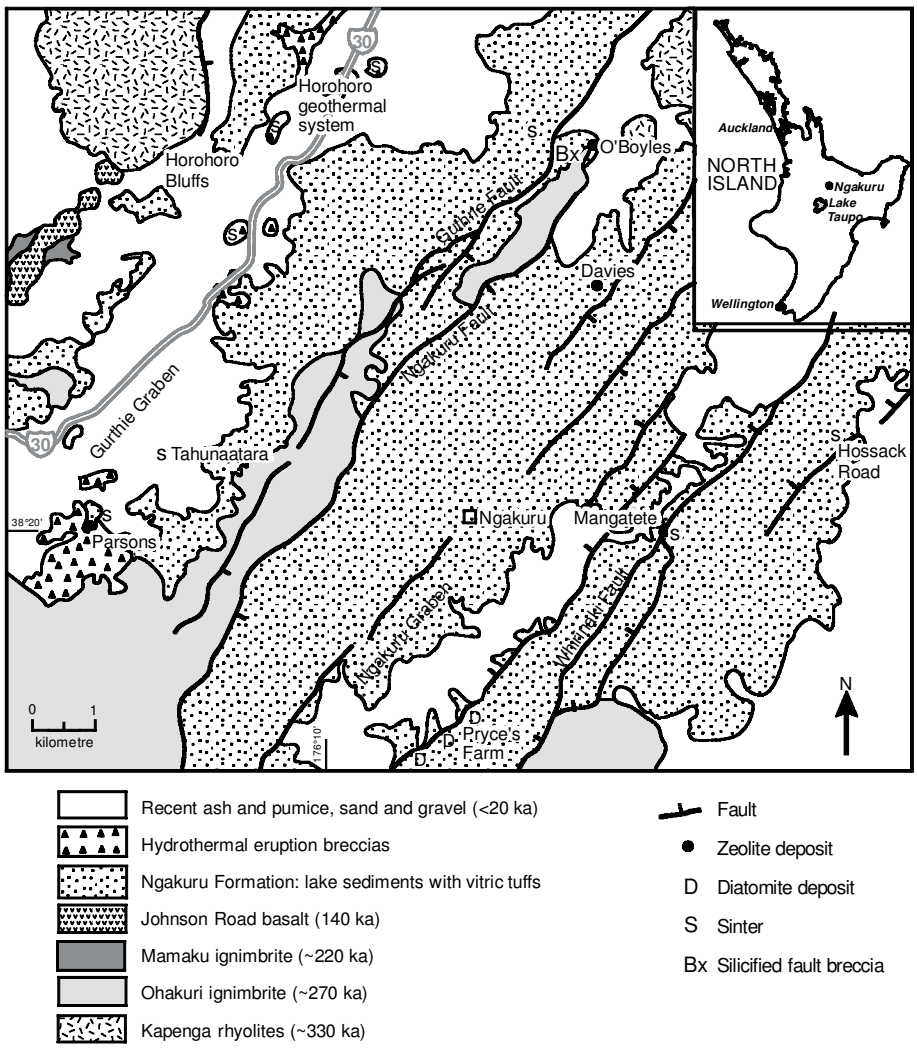

Figure 1. Geological map of the Ngakuru area, Taupo Volcanic Zone. Modified after Grindley (1960), Langridge (1990), Rutherford and Fransen (1990), Villamor and Berryman (2001), (C.P. Wood, pers. comm., 2001) and mapping by the author.

https://doi.org/10.1346/CCMN.2003.0510601 Published online by Cambridge University Press

The vitric tuffs of the Ngakuru Formation are composed mainly of glass shards and pumice clasts, with minor plagioclase, quartz and biotite crystals. Some beds contain pumice clasts and accretionary lapilli. Sedimentary structures such as load-casts and the thin mm–cm scale, laterally continuous, planar bedding, are consistent with deposition of airfall ash in a subaqueous low-energy environment. Diatomite-rich siltstones at Pryce's Farm (Figure 1) are up to 8 m thick, and were formerly (1958–1978) quarried for use as a pozzolan in lightweight concrete during building of hydroelectric dams on the nearby Waikato River. The Ngakuru Formation is unconformably overlain by traction-bedded alluvial sands and gravels of the Hinuera Formation, which are younger than ~20 ka (Figure 2).

Individual zeolite deposits contain 30–80% zeolite over thicknesses of up to 45 m in thinly stratified vitric tuff beds of the Ngakuru Formation. The zeolitic tuffs are white, in contrast to locally interbedded gray siltstones and mudstones. The primary components in the tuffs are glass shards and pumice clasts, with minor volcanic plagioclase, quartz and biotite crystals. A few of the vitric tuff beds contain accretionary lapilli. The Mangatete zeolite deposit is overlain by ~25 m of weakly silicified crystal-lithic tuffs and pumice-rich sand. There is a 2 m thick sinter capping the hill at the top of this sequence. Plant material in the sinter was extracted and dated at the Rafter Radicarbon Laboratory of the Institute of Geological and Nuclear Sciences, giving a ^{14}C age of 8498±60 BP.

At Parsons zeolite deposit, zeolitic tuff is interbedded towards the base with smectite-rich gray mudstone (samples 64970-71). A nearby sample (64976) from higher in the sequence is a diatomite. Hydrothermal eruption breccias in the vicinity of Parsons (Figure 1) overlie the Ngakuru Formation and contain clasts of altered Ohakuri Ignimbrite and Ngakuru Formation siltstone in a matrix that is locally altered to clay and pyrite. Wood fragments dated by ^{14}C indicated that the breccias are older than 45 ka (Langridge, 1990).

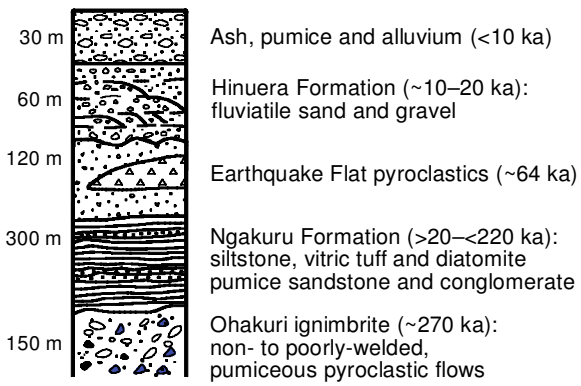

Figure 2. Reconstructed stratigraphic succession of the sedimentary and volcanic sequence in the Ngakuru area. Maximum thickness of units noted.

Hydrothermal eruption breccias have no primary volcanic components and are interpreted as the products of steam-driven eruptions (Nairn and Wiradiradja, 1980).

Bedding in the Ngakuru Formation is near flat-lying. The distribution of the formation is disrupted by still-active, northeast-trending normal faults, which separate it into the Ngakuru and Guthrie grabens (Figure 1) (Villamor and Berryman, 2001). A horst block of Ohakuri Ignimbrite separates these grabens. Rutherford and Fransen (1990) mapped a silicified hydrothermal breccia along the northern part of the Guthrie Fault.

MATERIALS AND METHODS

Thirty-two representative grab samples were collected from zeolite-bearing tuff, siltstone and ignimbrite occurrences in the Ngakuru area. The samples from the three quarried zeolite deposits (Mangatete, Parsons and Davies) were taken at vertical intervals of 3 to 5 m and are listed in Table 1 from the top down. The sample of diatomite (64976) was from a hillside outcrop near Parsons. The remaining samples of zeolitic tuff and ignimbrite listed in Table 1, are from road cuttings (O'Boyles) or hillside outcrops. Unaltered tuff and ignimbrite from the Ohakuri Ignimbrite, volcaniclastic sand from the Ngakuru Formation, hydrothermal breccias and sinters were sampled for petrographic examination.

X-ray diffraction

Zeolites and other minerals were identified by X-ray diffraction (XRD) analysis using a Philips X'Pert Pro (40 kV, 35 mA) with CoKα radiation. Mineral abundances, as listed in Table 1, were estimated with reference to an internal corundum standard. Oriented clay mounts of selected samples were successively analyzed under air-dried and glycerol solvated conditions to characterize the clay minerals. A Leo 440 scanning electron microscope (SEM) was used to examine the crystal habit, size and spatial relationships of the zeolites and other mineral. Chips ~10 mm in size were cemented on to 12 mm-diameter aluminum stubs and then coated with gold-palladium in carbon or carbon only. Semiquantitative chemical analyses were performed on selected crystals with a Link^{ISIS} system attached to the SEM in energy dispersive (EDS) mode at 20 kV (Table 2). Variations in density were measured on selected samples by standard hydrostatic weighing methods (Table 1). Porosity (water adsorption capacity) was also determined on the same samples. Whole-rock X-ray fluorescence (XRF) spectrometry analyses (Table 3) were performed by SpectraChem Analytical. Loss on ignition (LOI) was carried out at 1000°C for 1 h on samples dried for 3–4 h at 110°C. Following ignition and prior to reweighing, samples were cooled for 8–10 min in a Pyrex dessicator to prevent dehydration of the zeolites.

https://doi.org/10.1346/CCMN.2003.0510601 Published online by Cambridge University Press

Table 1. Mineral assemblages, densities and porosities of samples from Ngakuru.

Location	Sample	Lithology	Mo	Cl	K-fel	Op-A	Op-C	Sm	Q	Pl	Density (g cm^{-3})	Porosity (%)
Mangatete	64962	Tuff	C	M				M	T		1.2	48.1
Mangatete	64961	Tuff		C	M	C	C		T		1.1	44.6
Mangatete	64960	Tuff		C		M	C	M	M	T		
Mangatete	64959	Tuff	C		C	T		C	T	M		
Mangatete	64958	Tuff	C	C	T	T	M	T	T			
Mangatete	64957	Tuff	C	C	T	T	C	T	T			
Mangatete	64956	Tuff	C	C	M		M	T	M	T	1.0	52.1
Mangatete	64955	Tuff	C	C	M	T	M	T	M	T		
Mangatete	64954	Tuff	C	C		M	M		T		1.0	55.1
Mangatete	64953	Tuff	C	M		T	M	M	T			
Davies	64986	Tuff	A		M	C	M			T	0.66	72.6
Davies	64985	Tuff	A		M	M	T		T	T	0.97	56.5
Davies	64984	Tuff	A		M	M	M		T	T	0.87	62.1
Davies	64983	Tuff	A		M	C			T	T	1.12	43.4
Davies	64982	Tuff	A		M	M	T			T	0.88	60.5
Davies	64978	Tuff	A		T	T	M	T	T			
Davies	64979	Tuff	A		M	M	T	T	T			
Davies	64980	Tuff	A		M			M	T	M	0.87	60.5
Davies	64981	Tuff	A		M	M	T	T			0.89	60.0
O'Boyles	64987	Tuff	C		M	M	M	T	T			
O'Boyles	64988	Tuff	C		M	M	M	T	T			
O'Boyles	64989	Ignimbrite	A		M	M	M					
O'Boyles	64990	Ignimbrite	A			M	M		C	M		
Parsons	63977	Breccia	M	T	M	T			A	M		
Parsons	64976	Diatomite			M	M	A		T		0.84	61.9
Parsons	64975	Tuff	C	C	M				M	M		
Parsons	64974	Tuff	C		M	M		T	C		0.99	55.5
Parsons	64973	Tuff	C	M	M	T		T	M		1.03	53.7
Parsons	64972	Siltstone	M		C		M	C	M			
Parsons	64971	Siltstone	M		C	T	M	C	C			
Parsons	64970	Siltstone	M	T	M	T	M	C	M			
R. Plate Rd	64992	Tuff	A	M	T	C			T		1.33	42.5
Ohakuri	64995	Ignimbrite	C	M		C		T	T	C		
Ohakuri	64996	Ignimbrite	C	C	M			T	T	M		

Sample numbers refer to the National Petrology Collection held at the Institute of Geological and Nuclear Sciences. Mineral abbreviations: Cl = clinoptilolite, K-fel = K-feldspar, Mo = mordenite, Op-A = Opal-A, Op-C = Opal-CT, Pl = plagioclase, Sm = smectite, Q = quartz. Abundance abbreviations: A = abundant (>60%), C = common (60–20%), M = minor (20–5%), T = trace (<5%).

Table 2. SEM-EDS analyses of clinoptilolite, mordenite and K-feldspar from Ngakuru. Number of ions based on oxygen atoms as shown.

	Clinoptilolite					Mordenite		K-fel
Sample	64958a	64958b	64960a	64961a	64961b	64957a	64957b	64957c
Ions	72	72	72	72	72	96	96	32
Si	28.80	29.39	29.59	29.39	29.84	40.38	40.62	12.31
Al	7.67	7.00	6.66	6.46	6.08	7.71	7.38	3.77
Fe^{3+}	0.74	0.43	0.11	0.14	0.23	0.03	0.12	
Mg	0.29	0.27	0.25	0.29	0.29	0.27	0.36	
Ca	0.79	1.08	1.10	1.22	1.01	1.08	1.56	
Na	1.26	1.17	0.90	0.99	0.56	3.99	2.34	0.27
K	0.90	0.74	1.85	2.79	2.84	0.66	1.02	3.01
Si/Al	3.75	4.20	4.44	4.55	4.91	5.24	5.50	
Ca/K	0.88	1.45	0.60	0.44	0.36	1.64	1.53	
Ca/Na	0.63	0.92	1.23	1.23	1.80	0.27	0.67	

https://doi.org/10.1346/CCMN.2003.0510601 Published online by Cambridge University Press

RESULTS

Petrography and mineralogy

Vitric tuffs. Glass shards in the tuffs are replaced by zeolite minerals (Figure 3a), which consist of the silica-rich zeolites, mordenite and clinoptilolite (Table 1). Mordenite is generally more abundant than clinoptilolite and is the sole zeolite identified at Davies and O'Boyles. Amorphous silica (opal-A), opal-CT and K-feldspar are also present as secondary minerals. In SEM micrographs, mordenite occurs abundantly as a mesh of acicular crystals up to 15 μm long replacing the matrix of the tuffs (Figure 3a–b). As shown in Figure 3a, glass shards have been leached and the remaining molds are partly filled by acicular mordenite. This suggests that the process of zeolitization involved direct dissolution of glass and precipitation of mordenite. There is no evidence for the mordenite precipitation being preceded by the initial alteration of the glass to a clay mineral, as proposed for the zeolitization of volcanic glass in many sedimentary zeolite deposits by Leggo *et al.* (2001). Mordenite also occurs as hair-like fibers up to 200 μm in length that drape over crystals of clinoptilolite or K-feldspar (Figure 3c,e). This fibrous mordenite is late in the depositional sequence. Semiquantitative analyses by SEM-EDS of the acicular mordenite crystals indicate that it has Si/Al ratios of 5.2–5.5 and Ca/K of 1.5–1.6 (Table 2). Clinoptilolite occurs in tabular crystals 3–10 μm in the longest dimension (Figure 3c). It commonly lines open cavities of dissolved glass shards. Analyses by SEM-EDS indicate Si/Al ratios of 3.7–4.6 and Ca/K ratios of 0.4–1.5, which are both lower than those in the acicular mordenite.

Opal-CT forms tiny (<1 μm), thin-bladed crystals, which aggregate locally into small lepispheres (Figure 3d). Most of the samples contain K-feldspar in the range 5–30% from XRD. It occurs locally in the form of clusters of small (<5 μm) rhomb-shaped crystals (Figure 3e). The habit of the K-feldspar in the Ngakuru samples indicates an authigenic origin, similar to that found in zeolitized silicic tuffs elsewhere (*e.g.* Yucca Mountain, Nevada, Broxton *et al.*, 1987). Smectite is present in 'trace' to 'common' amounts, and the presence of the main peak at generally <14 Å in air-dried samples characterizes the smectite as a Na-rich smectite, consistent with derivation from rhyolitic volcanic ash. Some of the samples also contain trace to minor illite, which is probably of detrital origin.

Diatomite. The sample (64976) from above the zeolitic tuff at Parsons consists of diatom valves in a matrix of tiny (<1 μm) crystals of cristobalite (Figure 3f). From XRD analysis, this is mainly cristobalite (opal-C) with minor opal-A and K-feldspar. The main diatoms present are *Cyclostephanos dubius*, with minor *Epithemia ?adnata* (U. Cochran, pers. comm. 2002). Diatomite from Pryce's Farm is composed mainly of *Aulacoseira ambigua*, with minor *Cyclotella stelligera* (U. Cochran pers. comm., 2002). The diatoms at both localities are extant species that are present in lakes in the TVZ (Cassie, 1989). The diatomite at Pryce's Farm is unaltered and consists mainly of opal-A, and therefore the conversion to opal-C at Parsons is interpreted as being due to reaction with heated groundwater.

Ignimbrites. Zeolites also occur in the adjacent underlying Ohakuri Ignimbrite at O'Boyles (Table 1), with similar alteration mineral assemblages (mordenite + clinoptilolite + K-feldspar + Opal-A + Opal-CT) in ignimbrite and overlying vitric tuff. At the extinct Ohakuri hydrothermal system, 14 km southwest of Ngakuru, glass in the ignimbrite is hydrothermally altered to mordenite, clinoptilolite, K-feldspar, Opal-A and smectite (Table 1).

Hydrothermal fault breccia. Silicified hydrothermal breccia occurs along a fault zone near O'Boyles (Bx on Figure 1) and consists of fractured clasts of ignimbrite up to 5 cm long in a matrix of microcrystalline quartz. The glass matrix of the ignimbrite is also replaced by microcrystalline quartz (Figure 4), although relic shard textures are present. Plagioclase crystals are partly replaced along the rims and cores by adularia (Figure 4).

Hydrothermal eruption breccias. These breccias occur within the Guthrie Graben (Figure 1) and are considered to represent hydrothermal activity associated with the weakly active Horohoro geothermal system (Rutherford and Fransen, 1991). A sample (64977) that was analyzed using XRD and a petrographic microscope contains clasts of crystal-vitric tuff and thin-bedded vitric tuff in a matrix of comminuted rock and crystals that is locally altered to clay and pyrite. The tuff clasts contain mordenite, clinoptilolite and K-feldspar, a similar alteration assemblage to that in the underlying zeolitic tuffs at the nearby Parsons zeolite deposit. This suggests that the zeolitic alteration took place before the eruption of the breccias.

Sinters. Sinter sheets and mounds, together with silicified alluvial sands and gravels, are associated with hydrothermal eruption breccias in the Horohoro geothermal system and also occur above the Mangatete zeolite deposit and at Tahunaatara (Buddle, 2002) and Hossack Road (Holland, 2000) (Figure 1). In the Horohoro geothermal system, Rutherford and Fransen (1991) mapped recent and older (15–50 ka) sinters separated by alluvial sands and gravels.

Silicified volcaniclastic sands and lithic and crystal tuffs, with sinter at the top, overlie zeolitic tuff beds at the Mangatete zeolite deposit. The sinter is 2 m thick and has thin mm-scale laminae of white cherty silica interbedded with cm-thick layers of white plant stem fragments in a brown vitreous matrix. By analogy with

https://doi.org/10.1346/CCMN.2003.0510601 Published online by Cambridge University Press

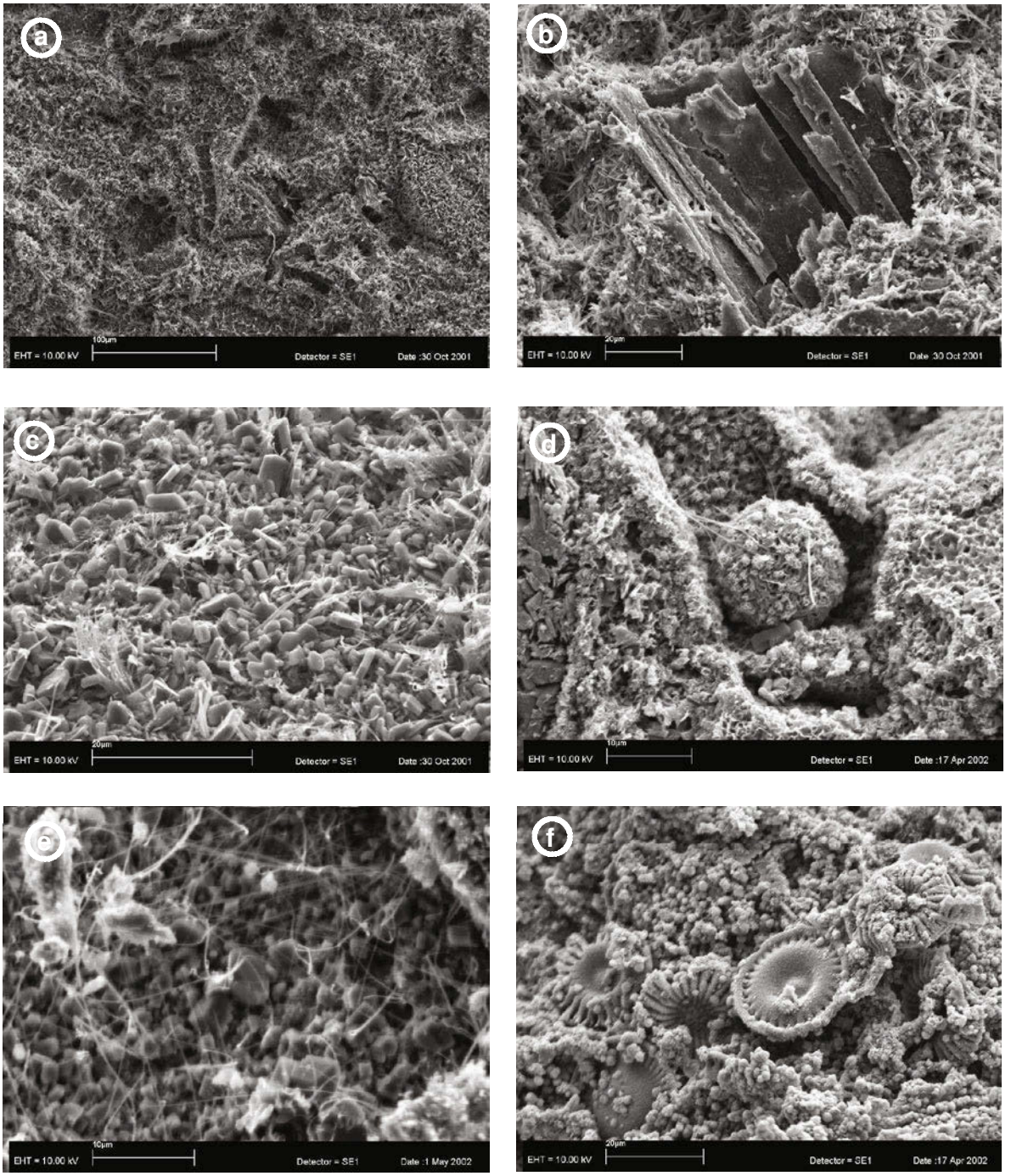

Figure 3. SEM images of minerals in tuffs and diatomite from Ngakuru. (a) Tuff from O'Boyles showing acicular mordenite crystals replacing matrix and partly filling molds of glass shards (curved). (b) Tuff from O'Boyles showing tubular pumice clast partly leached and enclosed by mordenite-rich matrix in tuff. (c) Tuff from Mangatete showing tabular crystals of clinoptilolite with minor fibrous mordenite. (d) Tuff from Mangatete containing minute thin-bladed crystals of opal-CT locally aggregated into a lepisphere, with a few clinoptilolite crystals below the lepisphere and several mordenite fibers. (e) Cluster of rhomb-shaped crystals of K-feldspar with minor fibrous mordenite. (f) Diatomite from Parsons composed of circular valves of *Cyclostephanos dubius* (Fricke) Round, in a matrix of tiny sphere-shaped crystals of Opal-C.

modern hot springs, these features are consistent with deposition in flowing water within and adjacent to hot water channels on spring mounds (Walter *et al.*, 1996).

Density and porosity

Density and porosity values are given in Table 1. Densities are mainly in the range 0.66–1.12 g cm^{-3}.

https://doi.org/10.1346/CCMN.2003.0510601 Published online by Cambridge University Press

Mordenite-rich samples generally have the lowest values (0.66–0.99 g cm^{-3}), whereas those containing clinoptilolite are higher (1.0–1.33 g cm^{-3}). The least dense (0.66 g cm^{-3}) sample is from the top of the Davies deposit. The diatomite sample (64976) has a similar density to the mordenite-rich samples. Measured porosity values are inversely related to densities and range from 44.6 to 72.6%.

The density values are very low compared with those of pure mordenite (2.1 g cm^{-3}) or with older zeolitic tuffs, *e.g.* 2.1–2.3 g cm^{-3} for Pliocene age zeolitic tuffs from Greece (Kitsopoulos and Dunham, 1996). The very low densities and correspondingly high porosities are due to the high void space, especially that created by the open mesh structure of the mordenite crystals (Figure 3a). These high porosities may partly be a function of the young age of the Ngakuru deposits, with consequent minimal compaction and cementation.

Whole-rock chemical composition

Whole-rock XRF analyses for 12 samples of vitric tuff are listed in Table 3. Since the tuffs consist mainly of altered volcanic glass, their original chemical composition should approximate that of the volcanic eruptive rocks from which they were derived. Elements that were immobile during zeolitic alteration should give an indication of the composition of the precursor volcanic rocks. A Zr/TiO_2-Nb/Y immobile element ratio plot (Figure 5), which discriminates the fields for volcanic rocks regardless of the effects of post-magmatic alteration (Winchester and Floyd, 1977), shows that the tuff analyses cluster around the boundary between rhyolite and rhyodacite/dacite. The unaltered vitric tuff (64993) from the Ohakuri Ignimbrite plots in the middle of the cluster of zeolitic tuff analyses.

Elements that were immobile during alteration may be used to discriminate the effects of hydrothermal alteration from those due to mixing and sorting in pyroclastic and volcaniclastic rocks (*cf.* Madeisky, 1996). Likely immobile elements Al, Ti, Zr and Y were plotted on *X-Y* graphs, and Zr *vs.* Al_2O_3 best meets the requirements of a linear trend (*i.e.* a constant ratio) through or near the origin for conserved elements that belong to a cogenetic igneous suite (Madeisky, 1996). As noted in several studies, Al is generally immobile in the alteration or diagenesis of zeolitized tuffs (Broxton *et al.*, 1987). To overcome the effects of closure on major element percent data, Pearce element ratios, expressed in molar terms, were calculated (method of Stanley and Madeisky, 1994; Madeisky, 1996). Plots of Pearce element ratios for possible mobile elements *vs.* the immobile element ratio Al/Zr, showed that only Na and K show significant variations (Figure 6b–c). The Si/Zr-Al/Zr plot (Figure 6a) exhibits a clear linear trend (slope of ~5), which matches that of rhyolites (Madeisky, 1996) and indicates that Si was not significantly mobile during the alteration. Plots for Fe/Zr, Mg/Zr and Ca/Zr *vs.* Al/Zr also showed linear trends, indicating that these elements were also immobile. These variations in Na and K and lack of variation in Fe, Mg and Ca are also evident from the analyses in Table 3. For analyses from the individual deposits, mordenite-rich tuffs (*e.g.* Davies zeolite deposit) generally have higher CaO and K_2O contents.

FORMATION OF THE ZEOLITE DEPOSITS

The presence of sinter, hydrothermal eruption breccias or silicified fault breccia in the vicinity of three of the zeolite deposits suggests that the zeolite deposits are associated with geothermal activity, similar to that at now active geothermal systems in the TVZ. The Wairakei geothermal system near Lake Taupo, contains

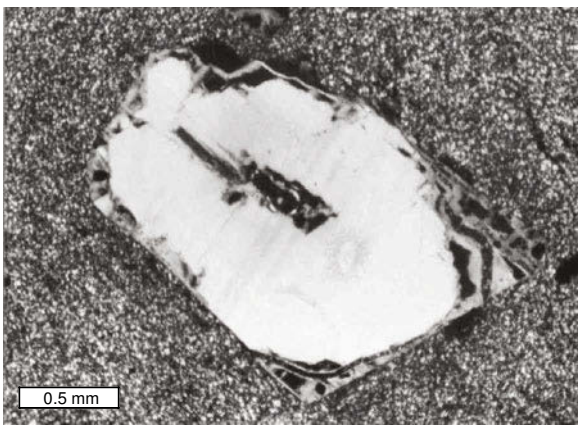

Figure 4. Photomicrograph of altered Ohakuri ignimbrite from silicified hydrothermal breccia in the Guthrie Fault zone near O'Boyles. Note primary plagioclase crystal replaced around the rim by adularia and the original glass matrix replaced by microcrystalline quartz.

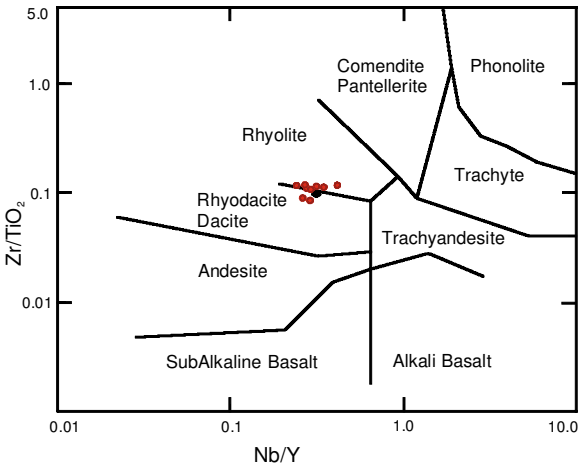

Figure 5. Plot of Zr/TiO_2 *vs.* Nb/Y for zeolitic tuffs from Ngakuru area, using XRF analytical data from Table 3. Fields for volcanic rock types from Winchester and Floyd (1977). Sample 64993 of unaltered vitric tuff from the Ohakuri Ignimbrite, lies in the middle of the data points.

https://doi.org/10.1346/CCMN.2003.0510601 Published online by Cambridge University Press

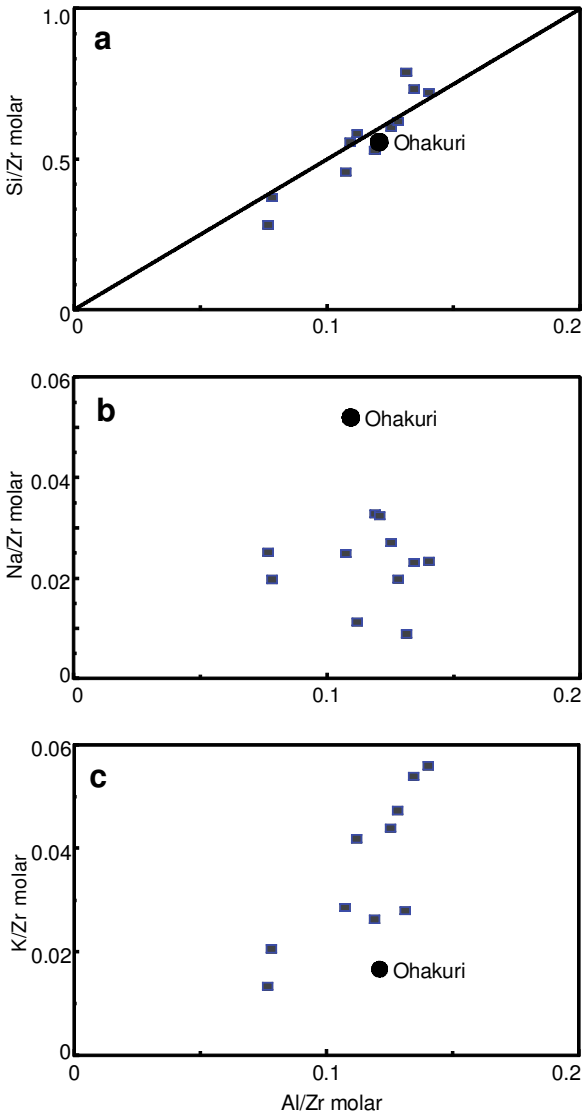

Figure 6. Variations in Si, Na and K for zeolitic tuffs, Ngakuru. (a) Plot of Al/Zr *vs.* Si/Al ratios. Line with slope = 5 is an average for rhyolites (*cf.* Madeisky, 1996). Sample Ohakuri is unaltered vitric tuff (64993). Any samples with Si enrichment would plot above the line and Si-depleted samples would plot below it. (b) Plot of Al/Zr *vs.* Na/Zr. (c) Plot of Al/Zr *vs.* K/Zr.

mordenite (Steiner, 1977) and clinoptilolite, which formed at temperatures of 60–160ºC, with mordenite forming at higher temperatures than clinoptilolite (C.P. Wood, pers. comm., 2001). However, detailed studies by Ma *et al.* (1995) of the alteration mineralogy of lacustrine tuffs and siltstones in the upper part of the Wairakei system lacustrine, indicate that mordenite and associated smectite were formed at temperatures <110ºC. The main fluid type at Wairakei and other similar geothermal systems is an alkali chloride water of near neutral pH and low salinity (0.2 wt.% NaCl) (*e.g.* Hedenquist, 1986). The main ions in the fluid are Cl, Na and K. In the extinct hydrothermal system at Ohakuri, the upper 100–150 m of the system is exposed. Henneberger and Browne (1988) described a central quartz + adularia + illite alteration zone grading outwards and upwards into a mordenite zone, characterized by a mordenite + clinoptilolite + smectite + opal assemblage (*e.g.* sample 64955). These authors reported that the mordenite-type alteration was accompanied by hydration of the host ignimbrite and inferred that it represented a zone of mixing of hot alkali-chloride water with cold groundwater.

By analogy, mordenite and clinoptilolite in the Ngakuru deposits probably formed at similar temperatures from groundwater-diluted, alkali-chloride water as a result of interaction with glass shards and pumice in the vitric tuffs. The mobile behavior of Na and K in the altered tuffs is further evidence for interaction between Na and K in the water and the rocks. The presence of authigenic K-feldspar is also consistent with mobilization of K during the alteration process. The Opal-CT probably represents the silica that was left over after the formation of mordenite and clinoptilolite from the glass shards, which, being of rhyolitic composition, are silica-rich (>70% SiO_2). The presence of opal-A, representing relict glass, in some samples suggests that alteration was incomplete in these samples. The quartz + adularia alteration observed in the hydrothermal breccia at O'Boyles, is likewise comparable to that in higher-temperature alteration zones below the mordenite-clinoptiloite zone in the Wairakei and Ohakuri systems.

The presence of silica sinters, such as that above the Mangatete zeolite deposit, implies deposition of sinter at the ground surface from heated alkali-chloride water of near-neutral pH (Herdianita *et al.*, 2000). The location of this sinter relative to the top of the zeolite alteration zone indicates that this zeolite deposit was formed at a shallow depth, *i.e.* 25 m to >70 m below the paleosurface.

The silicified hydrothermal breccia located in the Guthrie Fault zone at O'Boyles suggests that the fault acted as a feeder for heated alkali-chloride water that caused the deposition of the zeolite minerals. Because zeolites occur in vitric tuff clasts in the hydrothermal eruption breccias near the Parsons zeolite deposit, zeolitization there either predated, or was more likely contemporaneous with, the hydrothermal activity that resulted in eruption of the breccias. These breccias are older than 45 ka (Langridge, 1990), and the host vitric tuffs are older than ~64 ka (Villamor and Berryman, 2001). In the Ngakuru Graben, however, the host vitric tuffs are younger (~20 ka to >47 ka; Villamor and Berryman, 2001), and the age of zeolitization is ~8500 BP as indicated from the ^{14}C age of the sinter overlying the Mangatete zeolite deposit.

In summary, the Ngakuru zeolite deposits probably formed at shallow depth (<100 m) from reaction of glass-rich tuff beds with groundwater-diluted, alkali-chloride water of geothermal origin. There are some similarities with zeolite deposits formed by groundwater

https://doi.org/10.1346/CCMN.2003.0510601 Published online by Cambridge University Press

Table 3. Whole-rock XRF analyses of tuffs from Ngakuru.

	Ohak.	Mangatete				Parsons			Davies			
Sample	64993	64956	64958	64960	64961	64973	64974	64975	64982	64983	64984	64985
SiO_2 (%)	69.99	71.89	71.67	78.47	73.28	73.33	72.00	69.19	70.80	70.67	71.92	70.94
TiO_2	0.19	0.18	0.17	0.13	0.16	0.29	0.27	0.47	0.14	0.21	0.14	0.15
Al_2O_3	11.67	13.70	13.16	11.09	11.90	13.10	14.37	15.96	11.69	12.41	11.21	12.33
Fe_2O_3	3.34	1.61	1.19	1.39	0.83	1.12	1.34	1.74	1.17	1.41	1.07	0.87
MnO	0.06	0.03	0.02	0.06	0.04	0.02	0.01	0.02	0.01	0.02	0.01	0.01
MgO	0.34	0.31	0.39	0.37	0.34	0.32	0.32	0.31	0.17	0.18	0.16	0.16
CaO	1.00	1.25	1.82	1.16	1.81	1.64	1.30	2.35	2.01	2.05	1.93	1.87
Na_2O	3.37	2.29	2.15	0.46	0.73	2.00	2.02	3.18	1.19	1.63	1.17	1.16
K_2O	3.45	2.79	1.69	2.18	4.11	3.19	3.53	2.57	4.31	4.01	4.15	4.20
P_2O_5	0.04	0.01	0.01	0.02	0.01	0.02	0.02	0.02	0.02	0.02	0.02	0.02
LOI	6.33	5.62	7.35	4.34	6.22	4.53	4.76	4.14	8.31	7.09	7.93	7.91
Sum	99.77	99.68	99.61	99.67	99.43	99.55	99.94	99.95	99.81	99.69	99.72	99.62
Ba (ppm)	596	389	1232	765	1175	1178	656	524	637	624	633	644
Rb	116	170	193	118	258	135	185	116	133	123	128	135
Sr	75	57	115	65	131	220	157	245	90	103	91	92
Y	34	35	26	26	24	38	42	32	42	38	40	42
Zr	191	206	195	151	190	299	239	372	149	177	149	172
Nb	11	11	9	7	10	13	11	14	12	11	11	10
Th	10	11	10	6	13	12	10	10	14	12	12	13
Ga	14	19	14	12	13	16	20	18	14	14	13	14
Zn	50	55	71	51	56	48	50	51	37	45	35	38
Cu	5	4	2	3	2	3	3	1	3	3	2	1
Cr	11	3	<1	2	2	4	4	5	6	7	15	8
Sc	7	10	11	9	10	10	16	15	<1	<1	<1	<1
U	4	2	3	1	2	2	2	2	3	4	2	2
La	33	31	35	28	26	36	62	48	29	33	37	34
Ce	56	68	62	43	40	59	78	56	50	56	58	57

percolating through thick tephra deposits, *i.e.* the open hydrologic systems of Sheppard and Hay (2001) and others. However, the classic open hydrologic system deposits (*e.g.* John Day Formation, Oregon) are formed at much greater depths (300–450 m), and gentler thermal gradients, within thick sequences of silicic pyroclastic and volcaniclastic rocks of early- to mid-Tertiary age.

CONCLUSIONS

Zeolite deposits containing 30–80% zeolite occur over thicknesses of up to 45 m in rhyolitic vitric tuffs at Ngakuru in the Taupo Volcanic Zone. Mordenite and clinoptilolite have replaced glass shards and pumice in vitric tuffs that are the products of ash fall-out into a lake basin of late Quaternary age. The mordenite and clinoptilolite and associated authigenic K-feldspar and Opal-CT are very fine grained (generally <10 μm). The zeolitic tuffs have low densities, with values in the range 0.7–1.0 g cm^{-3} in mordenite-rich tuffs. The zeolite deposits are associated with sinter, hydrothermal eruption breccias and silicified fault breccias that represent surface or near-surface manifestations of geothermal activity. Plant material extracted from sinter overlying one of the zeolite deposits has a ^{14}C age of 8498±60 BP, indicating that the hydrothermal system that deposited the zeolites was recently active. By analogy with the occurrence of mordenite and clinoptilolite in some active geothermal systems in the TVZ, the Ngakuru zeolite deposits formed at shallow depths (<100 m) from reaction of glass-rich tuff beds with groundwater-diluted, alkali-chloride water of geothermal origin.

ACKNOWLEDGMENTS

I thank Craig Mowatt of New Zealand Natural Zeolite for information and access for sampling. Kay Card of Industrial Research Limited provided the expertise with the SEM. Ray Soong provided the XRD identifications, Christine Prior the ^{14}C date on the sinter, Phillip Warnes the density measurements, Neville Orr the thin-sections, and Ursula Cochran identified the diatoms. Thanks to Pat Browne, Darren Gravley, Andy Nicol, Agnes Reyes and Peter Wood for information and discussion. Tony Christie and Ian Graham reviewed a draft of the paper and Michelle Park assisted with the diagrams. This work was funded by the New Zealand Foundation for Research Science and Technology.

REFERENCES

Bibby, H.M., Caldwell, T.G., Davey, F.J. and Webb, T.H. (1995) Geophysical evidence on the structure of the Taupo Volcanic Zone and its hydrothermal circulation. *Journal of Volcanological and Geothermal Research*, **68**, 29–58.

Buddle, T.F. (2002) Sedimentary facies and mineralogy of the upper Pleistocene Tahunaatara sinter and associated depos-

https://doi.org/10.1346/CCMN.2003.0510601 Published online by Cambridge University Press

its. Unpublished MSc thesis, University of Auckland, New Zealand, 136 pp.

Broxton, D.E., Bish, D.L. and Warren, R.G. (1987) Diagenetic minerals at Yucca Mountain, Nevada. *Clays and Clay Minerals*, **35**, 89–110.

Cassie, V. (1989) A contribution to the study of New Zealand diatoms. *Bibliotheca Diatomologica*, Band 17. J. Cramer, Berlin-Stuttgart, 266 pp.

Grindley, G.W. (1960) *Sheet N85 – Waiotapu, Geological Map of New Zealand 1:63,360 scale*. DSIR, Wellington, New Zealand.

Hedenquist, J.W. (1986) Geothermal systems in the Taupo Volcanic Zone: their characteristics and relation to volcanism and mineralisation. Pp. 134–168 in: *Late Cenozoic Volcanism in New Zealand* (I.E.M. Smith, editor). *Royal Society of New Zealand Bulletin*, **23**.

Henneberger, R.C. and Browne, P.R.L. (1988) Hydrothermal alteration and evolution of the Ohakuri hydrothermal system. *Journal of Volcanological and Geothermal Research*, **34**, 211–231.

Herdianita, N.R., Browne, P.R.L., Rodgers, K.A. and Campbell, K.A. (2000) Mineralogical and textural changes accompanying ageing of silica sinter. *Mineralium Deposita*, **35**, 48–62.

Holland, G.R. (2000) The Whirinaki sinter, Taupo Volcanic Zone. Unpublished MSc thesis, University of Auckland, New Zealand, 115 pp.

Kitsopoulos, K.P. and Dunham, A.C. (1996) Heulandite and mordenite-rich tuffs from Greece: a potential source for pozzolanic materials. *Mineralium Deposita*, **31**, 576–583.

Langridge, R.M. (1990) The geology of the upper Atiamuri Region, Taupo Volcanic Zone. Unpublished MSc thesis, University of Waikato, New Zealand, 164 pp.

Leggo, P.J., Cochemé, J.-J., Demant, A. and Lee, W.T. (2001) The role of argillic alteration in the zeolitization of volcanic glass. *Mineralogical Magazine*, **65**, 653–663.

Ma, C., Browne, P.R.L. and Harvey, C.C. (1995) Clay mineralogy of sedimentary rocks in the Wairakei geothermal system. Pp. 399–404 in: *Clays: Controlling the Environment* (G.J. Churchman, R.W. Fitzpatrick and R.A. Eggleton, editors). *Proceedings 10th International Clay Conference, Adelaide, Australia, 1993*. CSIRO Publishing, Melbourne, Australia.

Madeisky, H.E. (1996) A lithogeochemical and radiometric study of hydrothermal alteration and metal zoning at the Cinola epithermal gold deposit, Queen Charlotte Islands, British Columbia. Pp. 1153–1185 in: *Geology and Ore Deposits of the American Cordillera* (A.R. Coyner and P.L. Fahey, editors). *Symposium Proceedings* Vol. III. Geological Society of Nevada, Reno, Nevada.

Manville, V. (2001) Sedimentology and history of Lake Reporoa: an ephemeral supra-ignimbrite lake, Taupo Volcanic Zone, New Zealand. Pp. 109–140 in: *Volcaniclastic Sedimentation in Lacustrine Settings* (J.D.L. White and N.R. Riggs, editors). Special Publication No. 30 International Association of Sedimentologists. Blackwell Science, Oxford, UK.

Mowatt, C. (2000) Preliminary investigations into characteristics and potential uses for Ngakuru zeolites. *2000 New Zealand Minerals and Mining Conference Proceedings*, Crown Minerals, Ministry of Economic Development, New Zealand, pp. 217–220.

Nairn, I.A. and Wiradiradja, S. (1980) Late Quaternary hydrothermal explosion breccias at Kawerau Geothermal Field, New Zealand. *Bulletin of Volcanology*, **43**, 1–13.

Roberts, P.J. (1997) Zeolite and silica. *1997 New Zealand Minerals and Mining Conference Proceedings*, Crown Minerals, Ministry of Commerce, New Zealand, pp. 199–203.

Rutherford, P.G. and Fransen, P.J.B. (1990) Final report on Kapenga EL 33495 Taupo Volcanic Zone. *Amax Resources NZ Ltd. Open-File Company Report*, Ministry of Commerce M2936, Wellington, New Zealand.

Rutherford, P.G. and Fransen, P.J.B. (1991) Timing of epithermal activity in the Horohoro-Matahana basin area, Taupo Volcanic Zone. *New Zealand Branch of the Australasian Institute of Mining and Metallurgy 25th Annual Conference Proceedings*, pp. 270–279.

Sheppard, R.A. and Hay, R.L. (2001) Formation of zeolites in open hydrologic system. Pp. 261–276 in: *Natural Zeolites: Occurrence, Properties, Applications* (D.L. Bish and D.W. Ming, editors). Reviews in Mineralogy and Geochemistry, **45**. Mineralogical Society of America, Washington, D.C.

Simmons, S.F., Browne, P.R.L. and Brathwaite, R.L. (1992) *Active and extinct hydrothermal systems of the North Island, New Zealand*. Society of Economic Geologists, Guidebook series vol. 15.

Smith, R.C.M., Smith, I.E.M., Browne, P.R.L. and Hochstein, M.P. (1993) Volcano-tectonic controls on sedimentation in the Taupo Volcanic Zone, New Zealand. Pp. 143–156 in: *South Pacific Sedimentary Basins. Sedimentary Basins of the World, 2* (P.F. Ballance, editor). Elsevier, Amsterdam, The Netherlands.

Stanley, C.R. and Madeisky, H.E. (1994) Lithogeochemical exploration for hydrothermal ore deposits using Pearce element ratio analysis. Pp. 193–211 in: *Alteration and Alteration Processes Associated with Ore-forming Systems* (D. Lentz, editor). Geological Association of Canada, Short Course Notes, **11**.

Steiner, A. (1953) Hydrothermal rock alteration at Wairakei, New Zealand. *Economic Geology*, **48**, 1–13.

Steiner, A. (1977) The Wairakei geothermal area North Island, New Zealand. *New Zealand Geological Survey Bulletin*, **90**.

Villamor, P. and Berryman, K. (2001) A late Quaternary extension rate in the Taupo Volcanic Zone, New Zealand, derived from fault slip data. *New Zealand Journal of Geology and Geophysics*, **44**, 243–269.

Walter, M.R., Desmarais, D., Farmer, J.D. and Hinman, N. (1996) Lithofacies and biofacies of mid-Paleozoic thermal spring deposits in the Drummond Basin, Queensland, Australia. *Palaios*, **11**, 497–518.

Wilson, C.J.N., Houghton, B.F., Lanphere, M.A. and Weaver, S.D. (1992) A new radiometric age for the estimate for the Rotoehu Ash from Mayor Island volcano, New Zealand. *New Zealand Journal of Geology and Geophysics*, **35**, 371–374.

Wilson, C.J.N., Houghton, B.F., McWilliams, M.O., Lanphere, M.A., Weaver, S.D. and Briggs, R.M. (1995) Volcanic and structural evolution of Taupo Volcanic Zone, New Zealand: a review. *Journal of Volcanological and Geothermal Research*, **68**, 1–28.

Winchester, J.A. and Floyd, P.A. (1977) Geochemical discrimination of different magma series and their differentiation products using immobile elements. *Chemical Geology*, **20**, 325–343.

(*Received June 2002; revised 31 January 2003; Ms. 684; A.E. David L. Bish*)